Photoactivation of ROS Production In Situ Transiently Activates Cell Proliferation in Mouse Skin and in the Hair Follicle Stem Cell Niche Promoting Hair Growth and Wound Healing

Elisa Carrasco[1,2,3,6], María I. Calvo[1,2,6], Alfonso Blázquez-Castro[1,2,7], Daniela Vecchio[3,4], Alicia Zamarrón[2], Irma Joyce Dias de Almeida[1,2], Juan C. Stockert[2], Michael R. Hamblin[3,4,5], Ángeles Juarranz[2] and Jesús Espada[1,2,6]

The role of reactive oxygen species (ROS) in the regulation of hair follicle (HF) cycle and skin homeostasis is poorly characterized. ROS have been traditionally linked to human disease and aging, but recent findings suggest that they can also have beneficial physiological functions in vivo in mammals. To test this hypothesis, we transiently switched on in situ ROS production in mouse skin. This process activated cell proliferation in the tissue and, interestingly, in the bulge region of the HF, a major reservoir of epidermal stem cells, promoting hair growth, as well as stimulating tissue repair after severe burn injury. We further show that these effects were associated with a transient Src kinase phosphorylation at Tyr416 and with a strong transcriptional activation of the prolactin family 2 subfamily c of growth factors. Our results point to potentially relevant modes of skin homeostasis regulation and demonstrate that a local and transient ROS production can regulate stem cell and tissue function in the whole organism.

Journal of Investigative Dermatology (2015) 135, 2611–2622; doi:10.1038/jid.2015.248; published online 30 July 2015

INTRODUCTION

The skin is the largest organ in mammals, consisting of three layers, epidermis, dermis, and hypodermis, with associated appendages, including hair follicles (HFs), sebaceous, and sweat glands. The biology of epidermal stem cells in the skin is well known (Blanpain and Fuchs, 2009; Baker and Murray, 2012). In particular, the pilo-sebaceous unit (HF and associated glands) and the HF growth cycle constitute a very well-characterized model to study the functional regulation of skin stem cells. The HF is a complex mini-organ that invaginates from epidermal sheets of the skin into the dermis (Muller-Rover et al., 2001; Baker and Murray, 2012; Gilhar et al., 2012). Hair production is the result of a cyclic activity of the HF alternating three sequential phases: anagen (growth), catagen (cessation and regression), and telogen (rest). The HF is divided into two main regions depending on size variation rates through the hair cycle: permanent and cyclic regions. The upper permanent region, composed of the infundibulum, associated glands, and the bulge, a major reservoir of HF stem cells, regulates the activity of the dermal papilla in the cyclic region (Ramos et al., 2013). Activation of the dermal papilla cells during the anagen phase promotes extensive cell proliferation and differentiation in the cyclic region, ultimately resulting in the formation and growth of the hair shaft. Skin components are constantly renewed by a stock of multipotent epidermal stem cells, which are located in the bulge region (Bg) of the HF and in the basal layer of the interfollicular epithelium (Blanpain and Fuchs, 2009; Baker and Murray, 2012).

Important and well-known molecular mechanisms, includ-ing Wnt/β-catenin, BMP/Tgfβ/Smad, PI3K/Akt, and ERK/MAPK signaling pathways (Baker and Murray, 2012; Lopez-Pajares

[1]Instituto de Investigaciones Biomédicas "Alberto Sols", Departamento de Bioquímica, CSIC-Universidad Autónoma de Madrid, Madrid, Spain; [2]Departamento de Biología, Facultad de Ciencias, Universidad Autónoma de Madrid, Madrid, Spain; [3]Wellman Center for Photomedicine, Massachusetts General Hospital, Boston, Massachusetts, USA; [4]Department of Dermatology, Harvard Medical School, Boston, Massachusetts, USA and [5]Harvard-MIT Division of Health Sciences and Technology, Cambridge, Massachusetts, USA

Correspondence: Jesús Espada, Instituto de Investigaciones Biomédicas "Alberto Sols", Departamento de Bioquímica, CSIC-Universidad Autónoma de Madrid, Darwin 2, Madrid 28049, Spain. E-mail: jespada@iib.uam.es

[6]Present address: Grupo de Dermatología Experimental, Instituto Ramón y Cajal de Investigaciones Sanitarias, Fundación para la Investigación Biomédica Hospital Universitario Ramón y Cajal, Carretera Colmenar Viejo Km 9.100, Madrid 28034, Spain.

[7]Present address: Aarhus Institute of Advanced Studies (AIAS), Høegh-Guldbergs Gade 6B Building 1630, room 113, Aarhus C 8000, Denmark

Abbreviations: AA, ascorbic acid; Bg, bulge region; BrdU, 5-bromo-2′-deoxyuridine; DHF-DA, 2′,7′-dichlorodihydrofluorescein diacetate; HF, hair follicle; LRC, label-retaining cell; mALA, methyl aminolevulinate; PBS, phosphate-buffered saline; PpIX, protoporphyrin IX; PT, phototreatment; ROS, reactive oxygen species

Received 18 February 2014; revised 26 May 2014; accepted 17 June 2015; accepted article preview online 2 July 2015; published online 30 July 2015

et al., 2013; Ramos et al., 2013), have key roles in the regulation of different aspects of skin stem cell and HF function. However, skin homeostasis and the HF cycle are extremely complex and multifactorial processes. Many of the interplaying mechanisms that govern and/or modulate the functional output of these processes are not well characterized. In particular, the potential physiological role of reactive oxygen species (ROS) in the skin is largely unknown.

The generation of ROS as by-products of essential and efficient metabolic reactions, such as cellular respiration or oxidase activity, is an inevitable biochemical side effect that can be extremely harmful for cell viability. The oxidative stress induced by the undesirable intracellular accumulation of ROS is a major cause of cell and tissue toxicity, and it is associated with several human diseases, including neurode-generative (Parkinson's, Alzheimer's, and Huntington's dis-eases), psychiatric (schizophrenia and bipolar disorder) and cardiovascular (stroke and myocardial infarction) disorders (Pieczenik and Neustadt, 2007; Valko et al., 2007). ROS are also implicated in sickle cell disease and the fragile X and chronic fatigue syndromes (el Bekay et al., 2007; Pieczenik and Neustadt, 2007). The so-called oxidative stress or free-radical theory of aging proposes a causal link between gradual, time-dependent ROS production during the whole lifetime and aging of the organism, a controversial theory that remains the subject of intense debate (Perez et al., 2009; Speakman and Selman, 2011).

Aerobic organisms have evolved powerful mechanisms to manage excess ROS production, and they are able to efficiently detoxify superoxide anions, hydroxyl radicals, hydrogen peroxide, and organic hydroperoxides into harmless H_2O and O_2. These mechanisms are exemplified by the superoxide dismutase, catalase, and glutathione peroxidase enzymatic systems (Machlin and Bendich, 1987; Fernandez and Videla, 1996; Mates and Sanchez-Jimenez, 1999). Interestingly, in the course of evolution, eukaryotic organisms have also developed systems to use ROS production for their own benefit. An example is the phagocyte, which is an essential cell player of the mammalian immune system that can produce radical oxygen and nitrogen species in a tightly controlled way to kill target pathogens (Klebanoff et al., 1983; Bylund et al., 2010).

Accumulated evidence suggests that eukaryotic cells can also actively promote the production of small amounts of ROS as part of signaling pathways that regulate cell survival and proliferation (Droge, 2002; Chiarugi and Cirri, 2003; Bartosz, 2009; Sena and Chandel, 2012). Furthermore, it has been reported that exogenous ROS can regulate stem cell function in in vitro systems (Le Belle et al., 2010). An abnormal ROS production has been also linked to the deregulation of intestinal stem cell proliferation that occurs during colorectal cancer initiation (Myant et al., 2013). These observations imply the existence of widespread ROS-dependent mechanisms for the regulation of cell function and tissue homeostasis. Here we have used the skin and the well-characterized epidermal stem cell niche located in the Bg of the mouse HF as a working model to provide a proof-of-concept for the hypothesis that a transient modulation of in situ ROS levels can regulate skin homeostasis and stem cell function in a whole organism.

RESULTS

Photodynamic treatment of mouse skin with methyl aminolevulinate and red light induces a transient in situ ROS production in the tissue

To this end, we first developed a reproducible method to promote a controlled and transient increase of ROS in the skin. High levels of intracellular ROS can be generated by a combination of light of an adequate wavelength and a photosensitizer (PS) in the presence of O_2 (Juarranz et al., 2008). The resulting photodynamic effect (Supplementary Figure S1A online) is widely used as a powerful cell killing method in clinical practice (photodynamic therapy) for the treatment of several skin diseases, including cancer and infections. At present, 5-aminolevulinic acid (ALA) or its methyl derivative (methyl aminolevulinate; mALA) in combi-nation with red light is the most widely used photodynamic therapy in the clinic. These compounds are not PS per se, but they function as precursors of the endogenous PS Proto-porphyrin IX (PpIX; Supplementary Figure S1B online; Juarranz et al., 2008).

We have previously demonstrated that mALA can be used to photogenerate tightly controlled low levels of intracellular ROS that are able to stimulate cell proliferation instead of cell death in cultured immortalized keratinocytes (Blazquez-Castro et al., 2012). Here, we have adapted this approach to mouse skin in vivo. We have evaluated irradiation doses from 2 to 10 J cm^{-2} and a fixed mALA concentration (25 mg Metvix, mALA 160 mg g^{-1} cream). We found that topical application of mALA on mouse dorsal skin promoted an extensive production and accumulation of PpIX in the tissue, as revealed by the characteristic reddish fluorescence of this compound under blue-light (407 nm) excitation (Figure 1a). As expected, mALA-dependent PpIX accumulation in the skin followed by 2.5 J cm^{-2} irradiation with red light (636 nm) to complete the photodynamic treatment (mALA+Light) resulted in a significant increase of in situ ROS levels in the tissue (Figure 1b). A time-course analysis showed that relative ROS production was transient, returning to initial levels 100 minutes after irradiation (Figure 1b). To gain further detail on the distribution of generated ROS in the tissue, we used the manageable mouse tail skin epithelium. Accordingly, experimental treatments and the localization of PpIX and ROS were evaluated ex vivo in whole pieces of the tissue. We established that incubation with mALA resulted in a significant accumulation of PpIX in the HF (Figure 1c), followed by a notable production of ROS after 10 J cm^{-2} of red-light irradiation (mALA+Light) that was detected to some degree all over the epidermis, including IFE, infundibulum, and sebaceous glands (Figure 1d). Notably, ROS signal rapidly disappeared or declined in most tissue locations, persisting for longer times in bulge cells (Figure 1d), which is the main niche or reservoir of epidermal stem cells in the skin. As these experiments were performed ex vivo to determine

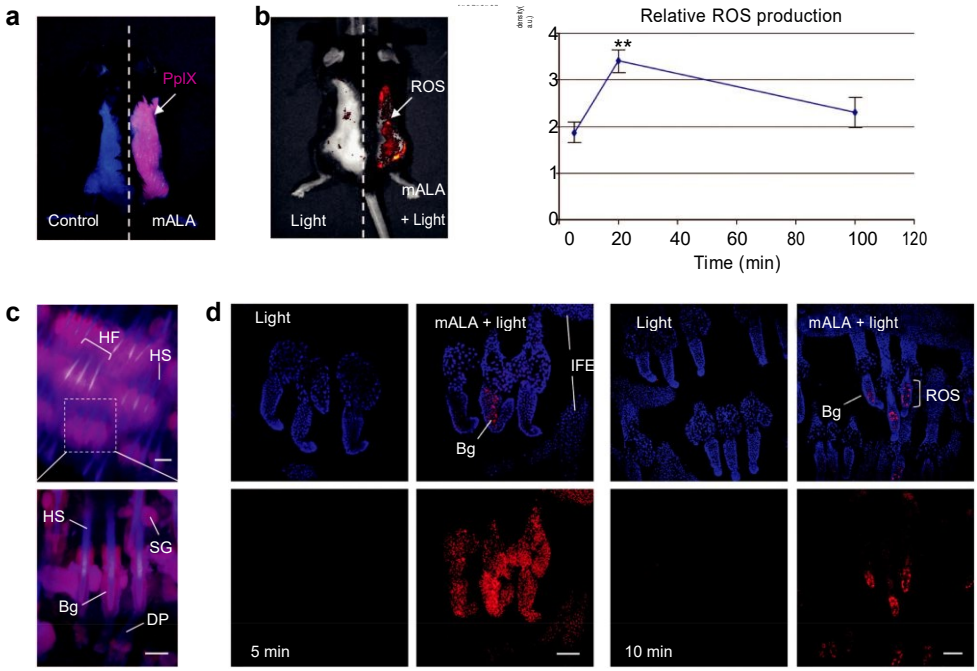

Figure 1. Photodynamic treatment with mALA and red light induces a transient production of ROS in the skin. (a) Accumulation of endogenous PpIX after mALA topic treatment in the back skin. The left side in the same animal was used as control. (b) Left panel: PpIX-dependent ROS (mALA+Light) production monitored by DHF-DA. Right panel: time-course analysis of relative ROS production in the back skin; the relative integrated density of DHF-DA fluorescent emission of mALA+Light versus Light regions in each animal was quantified at different times after irradiation and normalized as described in methodology. The mean ± SE was represented (n = 4 for each time point). (c) Localization of PpIX in the tail skin (fluorescence microscopy images). (d) ROS production in the tail skin after mALA+Light, as revealed by hET showing an increased and sustained accumulation in the bulge region of the hair follicle. Representative confocal microscopy images (maximum projections) are shown. Bars = 100 μm. DHF-DA, 2′,7′-dichlorodihydrofluorescein diacetate; hET, 2-hydroxyethidium; mALA, methyl aminolevulinate; PpIX, protoporphyrin IX; ROS, reactive oxygen species.

ROS localization, the time course of ROS production is not comparable to that observed in vivo in back skin. However, these results corroborate the transient nature of ROS produc-tion in the skin induced by our experimental approach, as well as the remarkable incidence on the bulge stem cell niche.

To rule out the deleterious effects of our protocol on cell and tissue viability, we used different approaches. We analyzed the formation of phosphorylated histone H2AX (pH2AX; also known as gammaH2AX) foci on the chromatin fibers that are associated with severe DNA damage (Yuan et al., 2010). No significant differences were observed in the number and distribution of pH2AX-positive cells in the skin in samples irradiated with red light after mALA application, as compared with light control samples (Supplementary Figure S2A online). In sharp contrast, a strong increase in the number of cells showing pH2AX foci was observed in UV-irradiated skin (Supplementary Figure S2A online). In the same way, we found that mALA+Light was unable to induce a noticeable increase in the number of apoptotic cells in the interfollicular epithelium or in the HF (Supplementary Figure S2B online). Finally, we also evaluated whether our protocol could alter the incidence of skin tumor formation. We performed two series of experiments involving a single mALA+Light (n = 5) or a dual treatment in a 15-day period (n = 3). In both cases, our results indicated that the mALA+Light treatment was completely safe and had no detectable or significant capacity to induce tumors in long-term experiments (up to 18 months).

Switching on in situ ROS production in the skin activates cell proliferation in epidermal and dermal layers and in the HF stem cell niche

We next investigated the potential effects of the transient ROS increase induced by mALA+Light on the function of epidermal stem cells in the Bg of the HF. To this end, we first proceeded to identify stem cells as label-retaining cells (LRCs) in pulse and long-chase experiments with the nucleotide analog 5-bromo-2′-deoxyuridine (BrdU; Braun et al., 2003). We quantified the number of LRCs in the Bg of HFs at 7 weeks after birth, during which time HFs are in a refractory telogen or resting phase of the growth cycle and are insensitive to stimulatory signals (Muller-Rover et al., 2001). We found that the transient in situ ROS production induced by mALA+Light activated the proliferation of bulge stem cells, promoting a significant increase in the number of BrdU-labeled cells, which was first detected in the skin 2 days after the treatment (Figure 2a). This was associated with a strong and parallel increase in the number of dividing (Ki67 positive) cells in the Bg (Figure 2b), indicating a proliferative response of the HF stem cell niche. The number of BrdU-labeled cells reverted to normal levels, as compared with control animals, 6 days after the treatment (Figure 2a), indicating the transient

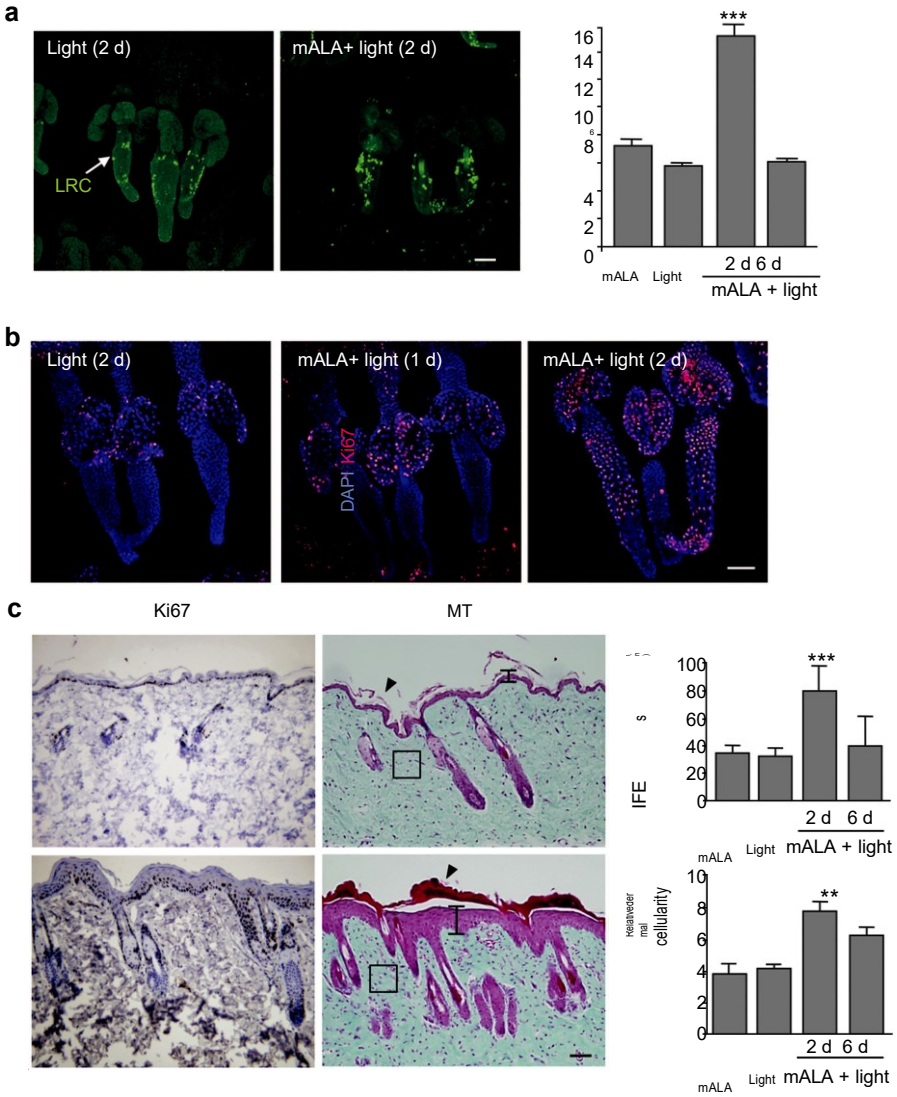

Figure 2. Switching on in situ ROS production in the skin activates stem cell proliferation in the hair follicle niche and promotes a transient proliferation of epidermal and dermal cells. (a) BrdU label-retaining cell (LRC) quantification in the hair follicle bulge region. The mean+SE (n = 4) is represented. (b) Immunological detection of the Ki67 proliferation marker in the hair follicle bulge region. (c) Dorsal skin histological sections stained for inmunohistochemical detection of Ki67 (left panels) or with Masson's trichrome (middle panels) showing transient effects in the skin induced by mALA+Light treatments, including cell proliferation, hyperplasia in the epidermis (vertical bars), a significant increase in dermal cellularity (squares), and strong cornification (arrowheads). Squares indicate equivalent areas in which cell numbers were quantified. Right panels show the quantification of interfollicular epidermis (IFE) thickness and dermal cellularity in 10 histological fields. The mean+SD (n = 3) is represented. In (a) and (b), representative confocal microscopy images (maximum projections) of tail epidermis whole-mounts are shown. Bars = 100 μm. mALA, methyl aminolevulinate; ROS, reactive oxygen species.

nature of the biochemical stimulus. These results were confirmed using a transgenic murine model in which GFP is expressed under the control of the keratin1-15 promoter, a molecular marker of HF epidermal stem cells (Morris et al., 2004). We found a significant increase of GFP-positive cells in the Bg of the HF 2 days after mALA+Light stimulus that returned to normal levels 6 days after the treatment (Supplementary Figure S3 online).

We also observed that mALA+Light promoted a transient increase in the number of proliferating cells in the epidermal and dermal layers of the skin starting 2 days after the treatment and returning to normal levels by day 6 (Figure 2c; Supplementary Figure S4A online). This proliferative pulse was associated with a transient epidermal hyperplasia and a significant increase of dermal cellularity 2 days after treatment that disappeared by day 6 (Figure 2c; Supplementary Figure S5C online). A strong cornification was also observed in treated skin regions (Figure 2c), suggesting an overall acceleration of tissue turnover rate. These processes were not associated with histopathological features of inflammation or with the induction of molecular skin inflammation markers, such as myeloperoxidase (MPO) (Figure 2c; Supplementary Figures S4B and S5C online). As a whole, these results are in agreement with our previous report in cultured keratinocytes

(Blazquez-Castro et al., 2012) and indicate that a transient production of ROS in the skin promotes a transient proliferative response in the tissue that can activate the epidermal stem cell niche.

Switching on in situ ROS production in the skin stimulates hair growth and accelerates burn healing

We reasoned that the effect of mALA+Light on cell proliferation in the skin and, particularly, on stem cells contained in the HF Bg should produce a physiological response in the target tissue. Supporting this concept, we observed that mALA +Light strongly promoted hair growth after shaving stimulation during the refractory telogen phase (Figure 3a; Supplementary Figure S5A online). Importantly, the use of antioxidant compounds such as ascorbic acid (AA) and N-acetylcysteine (NAC) abolished the differences in HF growth rates induced by mALA+Light with respect to Light control skin (Figure 3a and b; Supplementary Figure S5A online). In agreement with this observation, antioxidant treatment significantly inhibited the production of ROS (Figure 3a and c) and the activation of cell proliferation (Figure 3d) induced by mALA+Light in the tissue. It is to note that, as we have observed interindividual variations in the timing of hair growth in a day-range after the shaving stimulus, the comparisons between treated and control skin to quantify the mALA-phototreatment (mALA-PT) output were always established between different skin regions in the same mouse.

Morphological features and Lef1 expression in the hair germ indicated that anagen entry occurred about 6 days after treatments in mALA+Light-treated skin but not in the correlative light-treated skin controls or in nontreated skin (normal anagen) showing spontaneous anagen entry (Figure 3e). As expected, anagen entry was also observed in Light controls and in nontreated skin about 10 days after treatments as a consequence of shaving stimulation, showing Lef1 expression and cell proliferation in the hair germ and dermal papilla (Figure 3e and f). However, mALA+Light-treated skin consistently showed larger HFs with extensive cell proliferation at equivalent time points (Figure 3e and f). As a whole, these results indicate that a controlled and transient production of ROS in the skin can bypass the strong inhibitory signaling that occurs at refractory telogen of the HF cycle, forcing the premature entry into the anagen growth phase.

These results prompted us to investigate the ability of the transient ROS production to stimulate the regenerative potential of the skin. To this end, we performed a series of burn healing experiments. As shown in Figure 4, mALA+Light significantly accelerated the healing process after 2nd-degree burn injuries in the skin. Remarkably, this regenerative effect was associated with extensive cell proliferation in the Bg of HFs adjacent to the burned area (Figure 4d), indicating the activation of this stem cell niche. Taken together, these results suggest that the activation of skin proliferation and of the HF stem cell niche by a transient ROS production is a molecular signal able to stimulate different homeostatic programs in the skin, including hair growth and tissue regeneration.

Switching on in situ ROS production in the skin promotes a transient activating phosphorylation of cSrc kinase

We next sought to investigate the molecular mechanisms underlying the stimulation of skin induced by mALA+Light treatments. Since, as demonstrated above, this stimulation results in a transient proliferative wave 2 days after the treatment, returning to normal levels by day 6, we focused on this time period. We studied signaling pathways that are known to have key roles in the activation of epidermal stem cell function and HF growth, including Wnt/β-catenin, mitogen-activated protein kinases (MAPK), and PI3K/Akt signaling pathways. Interestingly, no changes in expression levels of either β-catenin or a metabolically stable, constitu-tively active form of this protein were detected after mALA +Light treatment (Figure 5a). Accordingly, no significant changes in the distribution of β-catenin were observed in mALA+Light-treated skin as compared with control samples, in both cases showing a major localization at the cell membrane and no nuclear translocation (Supplementary Figure S6A online), a key indicator of β-catenin-dependent transcriptional activation. As described above (Figure 3e) and as expected, Lef1 expression was found in HFs since day 6, and it was remarkable on advanced anagen, around 10 days after mALA-PT. In a similar way, no changes of phosphorylation at critical Thr/Tyr residues in different MAPK including JNK, p38, and ERK1/2, which are key indicators of signaling pathway activation, were observed after mALA+Light (Supplementary Figure S6B online). By contrast, a significant increase in phosphorylated Akt, similar to the increase observed in a neurosphere model (Le Belle et al., 2010), and a strong phosphorylation of Src kinase at Tyr416 were transiently detected 2 days after mALA+Light (Figure 5a). Interestingly, Src protein showed an increased accumulation in the epidermis of mALA+Light skin samples 2 days after treatment (Figure 5b) that disappeared at day 6 (Figure 5a). These results are consistent with our previous observations indicating a role for Src in the ROS-dependent induction of cell proliferation in human keratinocytes (Blazquez-Castro et al., 2012).

Switching on in situ ROS production in the skin induces a transient transcriptional activation of prolactin family 2 subfamily c members

To get a deeper insight into the molecular mechanism underlying the ROS-dependent, Src-driven activation of the epidermal stem cell niche, we performed a series of large-scale microarray analyses of mRNA expression, both in back and tail epidermis after mALA+Light as compared with control samples (GEO accession number GSE55135). Several genes showed significant transcriptional alterations 2 days after mALA+Light that were similarly modulated in tail and back epidermis (Table 1). It is to note that this large-scale analysis showed that mALA-PT was not associated with transcriptional profiles of inflammation or injury response. The transcriptional profiles of genes of interest were validated in all cases by quantitative real-time reverse-transcriptase– PCR in dorsal skin at both 2 or 6 days after mALA+Light (Figure 5c), revealing that the majority of genes transcription-ally altered at 2 days returned to normal expression levels

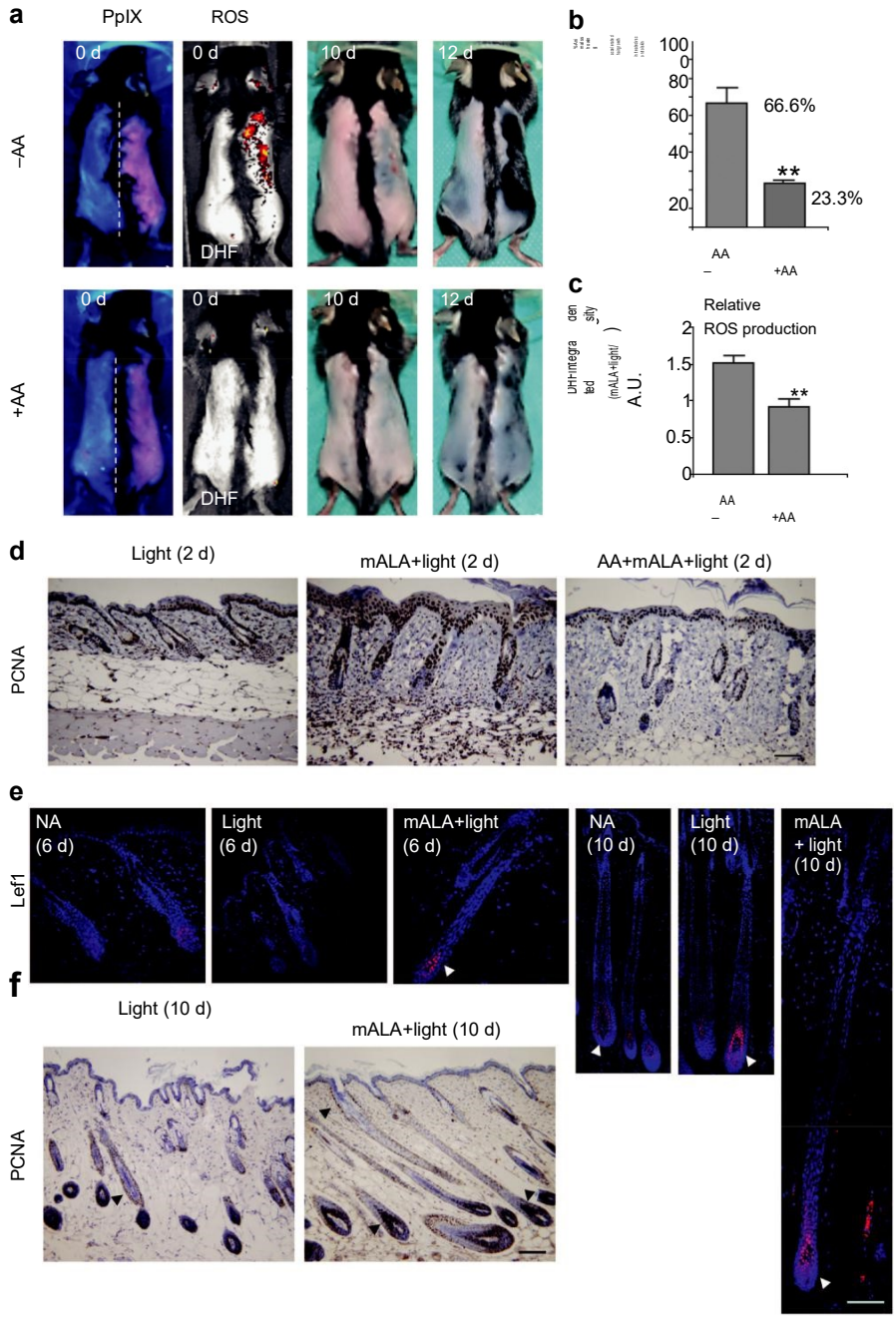

Figure 3. Switching on in situ ROS production in the skin stimulates hair growth. (a) Top row: Induction of hair growth during the refractory telogen phase by mALA+Light (right side of dorsal skin) as compared with Light control region (left side). Bottom row: Both ROS production in the skin and the acceleration of hair growth induced by mALA+Light were inhibited by AA antioxidant treatment. (b) Quantification of the percent of animals showing accelerated hair growth in mALA-PT as compared with the control region in the absence or presence of the antioxidant AA ($n = 4$ in 3 independent experiments). (c) Quantification of the ROS production inhibition in dorsal skin induced by AA during mALA-PT ($n = 4$, DHF-DA was applied 20 minutes after irradiation). (d) Inmunohistochemical detection of the PCNA proliferation marker in dorsal skin histological sections 2 days after mALA-PT showing inhibition of cell proliferation by the antioxidant AA. (e) Inmunolocalization of Lef1 (arrowheads) in equivalent hair follicle whole-length reconstructions generated from confocal microscopy images (maximum projections) 6 and 10 days after treatments in mALA+Light- and control Light-treated skin and in nontreated skin (normal anagen, NA). (f) Dorsal skin histological sections stained for inmunohistochemical detection of the PCNA proliferation marker 10 days after mALA-PT showing extensive cell proliferation in different regions of growing anagen hair follicles (arrowheads). Bars = 100 μm. AA, ascorbic acid; mALA, methyl aminolevulinate; PCNA, proliferating cell nuclear antigen; PT, phototreatment; ROS, reactive oxygen species.

6 days after the treatment. In agreement with our previous observations, targets of Wnt/β-catenin signaling in the skin, such as Jag1, Ovol1, and Axin2, were transcriptionally repressed 2 days after mALA+Light (Figure 5c). Interestingly, the strongest transient transcriptional activation induced by mALA+Light was observed for members of the prolactin family 2 subfamily c of growth factors. In particular, Prl2c3, also known as proliferin-2, showed a marked transient

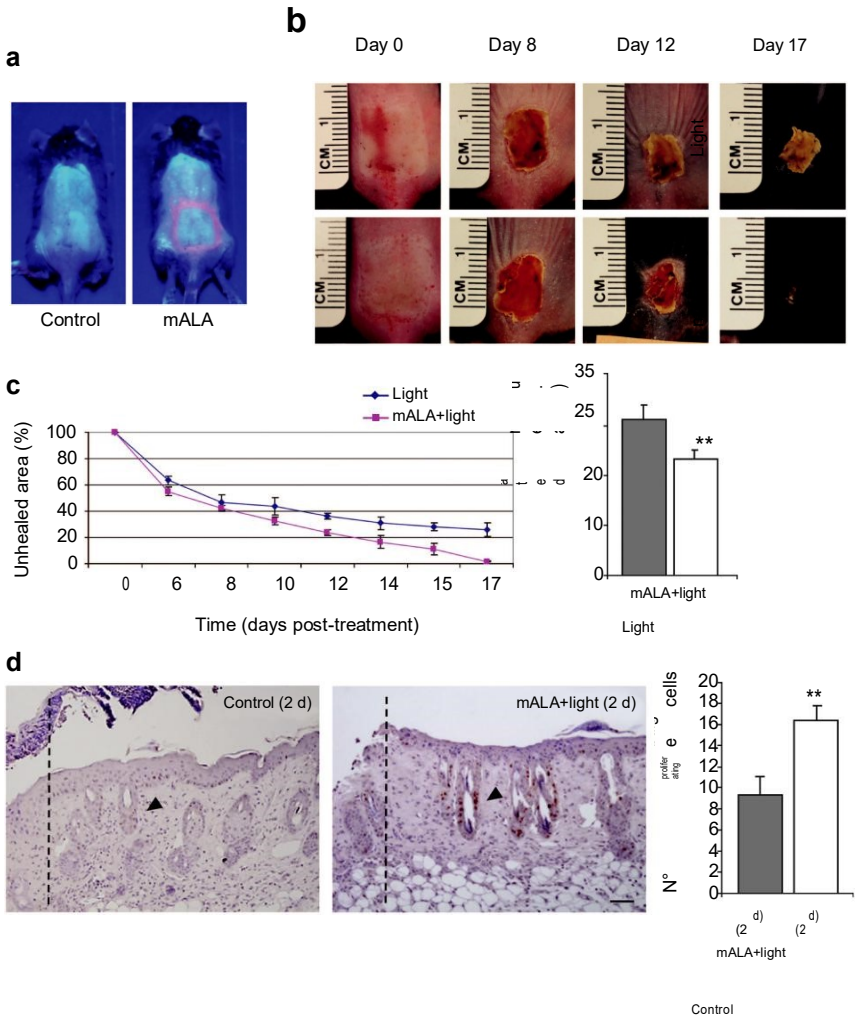

Figure 4. Switching on in situ ROS production in the skin accelerates burn healing. (a) PpIX production induced by mALA in burn injured regions in treated animals as compared with control samples. (b) Burn healing evolution in mALA+Light-treated and control animals. (c) Time-course quantification of burned areas (left panels) showing accelerated burn healing in mALA+Light-treated animals; the mean ± SE (n = 4) of unhealed area is represented. Area-under-the-curve analysis (right panels) demonstrating statistical differences between both time-course curves (P 0.06). (d) Histological images showing BrdU staining of proliferating cells in the bulge region (arrowheads) of hair follicles located in the adjacent area of the burn boundary (dotted lines) in mALA+Light as compared with control samples. Right panels: quantification of the number of proliferating cells in the three hair follicles closest to the burn boundary. The mean+SE (n = 3) is represented. Bar = 50 μm. BrdU, 5-bromo-2′-deoxyuridine; mALA, methyl aminolevulinate; PpIX, protoporphyrin IX; ROS, reactive oxygen species.

activation 2 days after switching on ROS production by mALA +Light (Table 1; Figure 5c). More surprisingly, we found a significantly increased expression of Prl2c3 protein in the skin associated with a strong nuclear localization in the hyper-plastic interfollicular epidermis (Figure 5d).

DISCUSSION

Here we have shown that switching on in situ ROS production can regulate functional responses in a tissue through the stimulation of cell proliferation and of a stem cell niche. Our results are in agreement with recent reports showing a role for ROS during the stimulation of neural stem cells in vitro in a neurosphere model (Le Belle et al., 2010) and in the deregulation of intestinal stem cell proliferation that occurs during colorectal cancer initiation (Myant et al., 2013). In these studies, an exogenous and/or continuous ROS supply or a systemic ROS depletion is used to evaluate a specific effect on a tissue or in biological systems. As a complement to these studies, our experimental approach implies a local and transient activation of in situ ROS production using the molecular machinery of the tissue. In this sense, our results are in close consonance with the observation that a transient ROS production occurs during tail regeneration in Xenopus tadpoles (Love et al., 2013). In this report, it is shown that activation of a regenerative signal, i.e., cutting the tadpole, is accompanied by a transient production of ROS. Here we demonstrate that switching on in situ transient ROS production activates a regenerative signal. It has also been reported that the mitochondrial transcription factor A (TFAM) is required for normal HF development and in vitro keratinocyte differentiation (Hamanaka et al., 2013), suggesting indirectly that mitochondrial ROS can have an important role in the regulation of skin function. Here we directly demonstrate that a transient generation of ROS in the

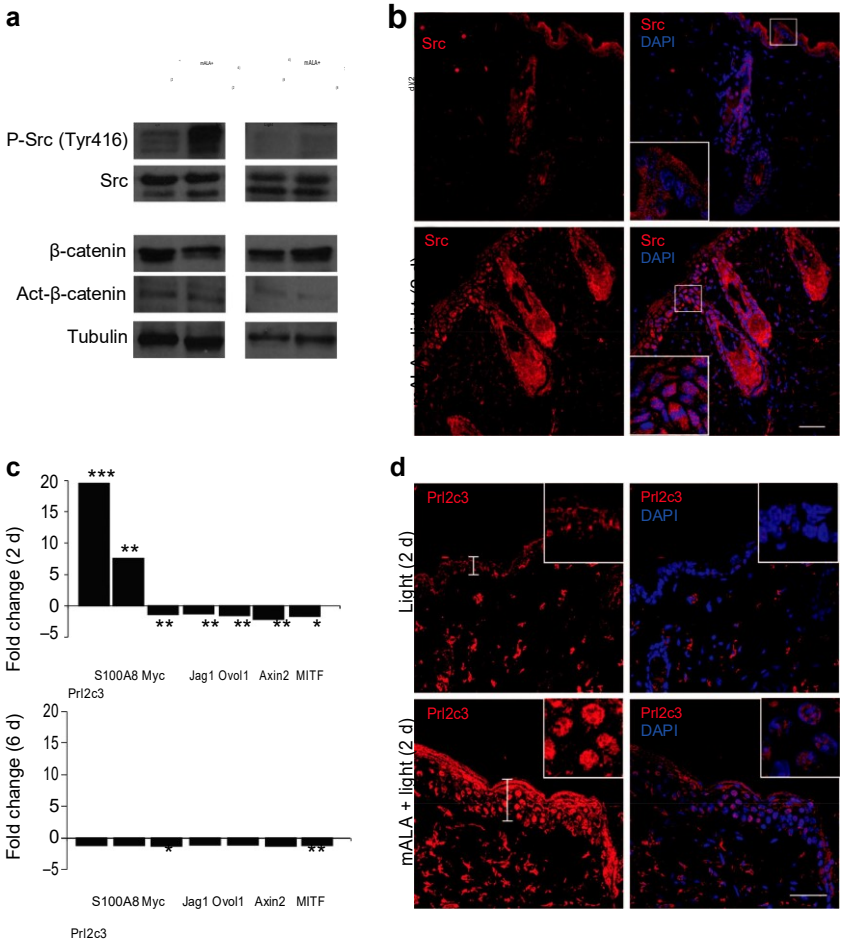

Figure 5. Molecular signatures associated with a transient switching on of ROS production in the skin. (a) Immunoblot analysis showing a transient phosphorylation of Src kinase in mALA+Light as compared with Light control samples in the back skin. (b) Transient Src kinase accumulation in the epidermis of mALA+Light samples. (c) Quantitative analysis of mRNA expression levels of the indicated genes in back skin. Fold change represents relative expression in mALA+Light with respect to control samples (***P 0.001, **P 0.05, *P 0.1). (d) Increased expression and nuclear translocation of Prl2c3 2 days after mALA +Light treatments. Inserts are detailed views of the nuclear distribution of Prl2c3 in epidermal keratinocytes. (b) and (d) correspond to representative confocal microscopy images (maximum projections). Bars = 50 μm. mALA, methyl aminolevulinate; MITF, microphthalmia-associated transcription factor; ROS, reactive oxygen species.

mouse skin activates the HF stem cell population, promoting hair growth in the refractory telogen phase and accelerating burn healing. In this context, it would be interesting to evaluate the clinical potential of a transient ROS production in situ in the skin to stimulate tissue homeostasis—e.g., to improve the healing process of small burns and chronic wounds or to activate hair growth or prevent hair loss in certain types of alopecia.

We have found that switching on in situ ROS production by mALA-PT promotes a transient proliferative pulse in the tissue, including bulge cells, 2 days after the treatment. This proliferative burst results in extensive anagen development of HFs by days 8–10, showing extensive cell proliferation and Lef1 expression particularly in the hair germ, and subsequent hair growth by days 12–19 after mALA-PT. At day 2, most HFs are in telogen and, consequently, no evidence of β-catenin accumulation or transcriptional activation of Wnt/β-catenin signaling is observed. However, a significant activating phosphorylation of cSrc occurs at this time point. This result is particularly interesting, as no significant roles are usually assigned to Src kinase in relation to the regulation of skin stem cell function and/or the HF growth cycle. However, it has been reported that Src protein expression and activity are regulated during normal HF cycle (Serrels et al., 2009). In the same context, the molecular mechanisms regulating Src kinase activity by ROS in cultured cells are well characterized (Giannoni et al. , 2010). These observations suggest that Src activity, independently or in combination with a controlled ROS production, can be an important partner in the skin signaling network, which merits further investigation. In this context, we hypothesize that mALA-PT induces, 2 days after treatment, an initial, cSrc-dependent, proliferative wave in the skin that is able to activate HF stem cell niches. This activation results in standard, Lef1-depen-dent, anagen entry around 6 days after treatments.

Table 1. Genes significantly up- or downregulated 2 days after mALA-PT in both back and tail epidermis

Gene	Access no. GenBank	Expression ratio	Associated functions
Prl2c3	NM_011118	(+) 144.93	Hormone-like growth factor. Putative role in wound healing and hair follicle cycle.
S100a8	NM_013650	(+) 25.55	Calcium- and zinc-binding protein, which has a wide plethora of intracellular and extracellular functions, including the modulation of the NADPH-oxidase activity and a role as an oxidant scavenger, respectively.
Gsta4	NM_010357	(+) 21.24	Conjugation of reduced glutathione to a wide number of exogenous and endogenous hydrophobic electrophiles.
Hip1	NM_146001	(+) 16.78	Plays a role in clathrin-mediated endocytosis and trafficking. Proapoptotic protein. May be required for differentiation, proliferation, and/or survival of somatic and germline progenitors.
Sox5	NM_011444	(+) 11.73	TF that has a role in cell lineage establishment during the development.
Fgf7 (Kgf)	NM_008008	(+) 4.40	Growth factor active on keratinocytes. Important role in the regulation of cell proliferation and differentiation.
Lef1	NM_010703	(+) 3.81	Participates in the Wnt signaling pathway. May have a role in hair cell differentiation and follicle morphogenesis.
Lrp1	NM_008512	(+) 3.15	Endocytic receptor involved in endocytosis and in the phagocytosis of apoptotic cells. May modulate cellular events, such as kinase-dependent intracellular signaling.
Tln2	NM_001081242	(+) 3.11	Major component of focal adhesion plaques that links integrin to the actin cytoskeleton.
Gapdh	NM_008084	(+) 3.07	Has both glyceraldehyde-3-phosphate dehydrogenase and nitrosylase activities, thereby playing a role in glycolysis and nuclear functions, respectively.
Myh4	NM_010855	(+) 2.79	Muscle contraction.
Fgf18	NM_008005	(+) 2.38	Important role in the regulation of cell proliferation, cell differentiation and cell migration. Stimulates hepatic and intestinal proliferation.
Cdh11	NM_009866	(−) 2.62	Calcium-dependent cell adhesion protein (homophilic interactions).
Bmp2	NM_007553	(−) 3.14	Induces cartilage and bone formation.
Notch2	NM_010928	(−) 3.14	Functions as a receptor for membrane-bound ligands Jagged1, Jagged2, and Delta1 to regulate cell-fate determination.
Rora	NM_013646	(−) 3.16	Orphan nuclear receptor. Regulates a number of genes involved in lipid metabolism, in cerebellum, and photoreceptor development in circadian rhythm and skeletal muscle development.
Myc	NM_010849	(−) 3.31	TF involved in the regulation of cell proliferation and cell differentiation of stem cells.
Mest	NM_008590	(−) 4.31	Belongs to the AB hydrolase superfamily. Expressed in the mesodermal tissues.
Pcaf	AF254442	(−) 4.35	Functions as a histone acetyltransferase (HAT) to promote transcriptional activation.
Ikzf4	NM_011772	(−) 5.03	DNA-binding protein that binds to the 5′-GGGAATRCC-3′ Ikaros-binding sequence. Interacts with SPI1 and MITF.

Abbreviation: mALA, methyl aminolevulinate; MITF, microphthalmia-associated transcription factor; TF, transcription factor. The expression ratios obtained by microarray analysis are referred to fold changes of mRNA expression in mALA+Light as compared with control samples. Associated functions were extracted from UniProt KB.

We have further shown that transiently switching on ROS production in the skin promotes a strong and unexpected transcriptional activation of prolactin family 2 subfamily c gene members, particularly Prl2c3. Surprisingly, we found that Prl2c3 was significantly translocated to the nucleus in most cell layers in the hyperplastic epithelium after mALA+Light treatment, suggesting that this hormone-like protein can have nuclear functions. Interestingly, it has been reported that this mitogen is expressed in the HF anagen growth phase (Fassett and Nilsen-Hamilton, 2001), and it facilitates the expansion of hematopoietic stem cells ex vivo (Choong et al., 2003). The role of Prlc3 in the skin is currently under investigation. In this context, the procedure presented here to transiently activate endogenous ROS production in the skin has been proven to be an efficient tool not only to suggest a physiological role for ROS in vivo but also to identify new signaling pathways and factors potentially implicated in the regulation of skin homeostasis.

MATERIALS AND METHODS

Animals

Seven-week-old C57BL/6 mice, including the strain B6.Cg-Tg(Krt1-15-EGFP)2Cot/J (Morris et al., 2004), were used. When possible, littermates were included in each experiment and comparisons were made between animals of the same sex. Both male and female mice were used in experiments using tail skin. Only female mice were used in experiments performed in the back skin. All animal husbandry and experimental procedures were conducted in compliance with 2010/63/UE European guideline or approved by the

Subcommittee on Research Animal Care (IACUC) of Massachusetts General Hospital (Boston, MA), in accordance with the guidelines of the National Institutes of Health (NIH).

Identification of LRCs in tail skin epithelium

Long-term BrdU (Sigma-Aldrich, St. Louis, MO) LRCs were generated and characterized as previously described (Braun et al., 2003). Briefly, 10-day-old mice were injected intraperitoneally once a day during four consecutive days with 50 mg per kg body weight BrdU dissolved in phosphate-buffered saline (PBS). After the labeling phase, mice were allowed to grow until the age of 7 weeks before any treatment. To prepare wholemounts of the tail epidermis, tails were clipped, skin was peeled from tails and incubated in 5 mM EDTA in PBS for 4 hours at 37 °C. Intact sheets of the epidermis were separated from the dermis using forceps and fixed in 4% formaldehyde in PBS.

Burning procedure

For induction of burn injuries, mice were anesthetized and shaved. A brass bar (1 cm in cross-section) that was preheated (~95 °C) by immersing in boiling water was applied on the dorsal surface of each mouse and maintained in contact with the skin for 5 seconds. The resulting nonlethal, partial-thickness, 2nd-degree burns measured ~ 1.3 × 1.3 cm. For the analysis of proliferating cells around the wound, animals received 2 sequential intraperitoneal injections of 50 mg per kg body weight BrdU every 12 hours, starting 4 hours after mALA-PT.

Photodynamic treatments

All experiments were performed during the refractory telogen phase of the HF growth cycle (7-week-old mice). For photodynamic treatments, mALA as topical cream (Metvix, Galderma, Lausanne, Switzerland) was used. For tail skin experiments, Metvix was applied directly on the skin. For back skin treatments, animals were completely shaved with a hair clipper and depilatory cream (Veet, Hull, UK) and washed with PBS. We applied 25 mg of Metvix covering the area of interest. After 2.5 hours of incubation in darkness, animals were anesthetized and the accumulation of PpIX was evaluated in situ by measuring the characteristic red fluores-cence under 407-nm blue-light excitation. To conduct the photo-dynamic treatments (mALA+Light), a red-light (636 nm) emission was subsequently applied on the dorsal surface of the tissue to a total dose of 2.5–10 J cm $^{-2}$, using a LED lamp (Aktilite, Photocure ASA, Oslo, Norway). Light control animals received only red light, whereas Dark control animals received only mALA and they were kept in the dark for at least 48 hours after the treatment. For inhibitory experiments using AA (from Sigma, St. Louis, MO), two doses of 100 mg/ml AA in 50% ethanol spaced 30 minutes were topically applied on the skin between the application of mALA and red-light irradiation. For the alternative experiments using NAC (from Sigma), a solution containing 20 mg ml $^{-1}$ NAC in PBS was intraperitoneally inoculated daily during 5 days at a dose of 100 mg per kg body weight, until the day that mALA-PT was applied. Photodynamic treatments on burned skin were performed 24 hours after the burning procedure. In all cases, the percent of animals showing hair growth acceleration in treated back skin regions as compared with control regions in the same animal was evaluated. An animal showing hair growth acceleration was defined as an animal showing full hair growth all along the treated region, typically by days 12–19 after shaving, but only limited or no hair growth in the control region.

Monitoring ROS production

ROS production in tail skin was evaluated ex vivo using hydro-ethidine (Sigma-Aldrich), which reacts with ROS to produce fluorescent dye 2-hydroxyethidium. Samples were incubated at 37 °C for 3 hours in a solution with 5 mM EDTA in PBS, containing 2 mM mALA in the case of treated samples. Hydroethidine was added to a final concentration of 3.2 μM. After 1 hour, the skin was irradiated with 10 J cm $^{-2}$ of 636-nm light and fixed.

For in vivo detection of ROS produced in back skin during photodynamic treatment, the ROS-sensitive 2′,7′-dichlorodihydro-fluorescein diacetate (DHF-DA; Sigma-Aldrich) was used. To assess the inhibitory effect of AA, two independent groups of animals were established for each time point for normalizing the obtained signal (mALA+Light/Light) with respect to AA animals. After dorsal skin shaving and PT treatment application, as previously described (Metvix 2.5 hours in dark followed by the irradiation with 2.5 J cm $^{-2}$ of 636 nm light), 1 mg ml $^{-1}$ DHF-DA in 50% ethanol was topically applied on the tissue at different time points after the irradiation (5, 20, and 100 minutes). ROS levels generated in the skin were determined 45 minutes after the application of DHF-DA in all cases, using an IVIS Lumina 2 imaging system (Xenogen, Alameda, CA), by measuring the fluorescent signal emitted by the fluorescein produced through the oxidation of DHF-DA. The filter settings were 445– 490 nm for the excitation and 515–575 nm for the emission.

Immunological and histological methods

Primary antibodies used were FITC-conjugated mouse monoclonal anti BrdU (Roche, Madrid, Spain); rabbit monoclonal antibodies against Src, Phospho-Src (Tyr416), AKT, Phospho-AKT (Ser473), p38 MAPK, Phospho-p38 MAPK (Thr180/Tyr182), p44/42 MAPK, Phos-pho-p44/42 MAPK (Thr202/Tyr204), Phospho SAPK/JNK (Thr183/ Tyr185), and gammaH2AX (Ser 139) and Lef1 (all from Cell Signaling Technologies, Leiden, The Netherlands); rabbit monoclonal anti Ki67 (Neo Markers, Fremont, CA); rabbit polyclonal anti Src (Abcam, Cambridge, UK); mouse monoclonal anti β-catenin (BD, Franklin Lakes, NJ); mouse monoclonal anti Active-β-catenin (Millipore, Billerica, MA); goat polyclonal anti-Proliferin 2 (Prl2c3) and anti-MPO (both from Santa Cruz Biotechnology, Dallas, TX); and mouse monoclonal antibodies against PCNA (Calbiochem, Billerica, MA), tubulin, and BrdU (both from Sigma).

For BrdU-FITC immunostaining in tail skin epithelium whole-mounts, fixed epidermal pieces were sequentially treated with 1 N HCl for 45 minutes at 37 °C and Tris-borate-EDTA for 5 minutes at room temperature and washed abundantly with distilled water. Permeabilization and blocking were carried out by incubation with PTG buffer (PBS containing 0.5% Triton X-100 and 0.2% gelatin) for 30 minutes at room temperature. Next, the samples were incubated with the FITC-conjugated primary antibody against BrdU (Roche) diluted 1:50 in PBS, overnight at 37 °C. For fluorescence immunos-taining of pH2AX, positive control samples were obtained from animals exposed to a total dose of 7.44 J cm $^{-2}$ of UVB light, using a lamp with a 312-nm emission peak (Philips TL, Eindhoven, The Netherlands, UV). Apoptosis was detected in whole-mounts using the TUNEL detection kit (Roche) according to the instructions of the manufacturer. Images were obtained in Leica TCS SP2 AOBS

spectral confocal microscope and processed using the FIJI software (Image J 1.49 National Institutes of Health, Bethesda, MD).

For immunohistochemical staining, hydrated paraffin samples were treated with trypsin (Thermo Scientific, Waltham, MA) for 30 minutes at 37 °C before incubating overnight with primary antibodies, and it was revealed using the Envision Flex/HRP (Dako, Barcelona, Spain) secondary antibodies cocktail and DAB kit (Vector Laboratories, Peterborough, UK).

For immunobloting, skin samples were homogenized at 4 °C in cold NT lysis buffer (50 mM Tris-HCl, pH 7.4, 100 mM NaCl, 5 mM $MgCl_2$, 5 mM $CaCl_2$, 1% NP-40, 1% Triton X-100, 2 mM phenylmethyl-sulfonyl fluoride, 20 μg/ml aprotinin, and 1 mM sodium orthovanadate).

RNA extraction and gene expression analysis

RNA was isolated from back skin and back and tail epidermis with TriPure Isolation Reagent (Roche) and the RNeasy Mini kit (Qiagen, Barcelona, Spain). Gene expression signatures were characterized using standardized mouse global mRNA expression arrays (Agilent Technologies, Santa Clara, CA; Agilent.SingleColor.14868). Gene expression analysis included pooled samples ($n = 3$) obtained 2 days after the treatment. Pools prepared from both back and tail epidermis were independently analyzed. Large-scale gene expression results were validated by quantitative real-time reverse-transcriptase–PCR in back skin samples. Primer sequences are available upon request.

Statistical analysis

Quantifications of LRC and Krt1-15-GFP expression in the Bg were performed on confocal images (30 HFs/animal, 3 animals/group). BrdU-positive cells were quantified in the three HFs closest to the burned area in 3 different animals per condition. Comparisons between groups were performed by Student's *t*-test using the SPSS 15.0 software (IBM, Spain). Skin thickness was measured in 10 different regions of the interfollicular epidermis per mouse including 3 animals per condition.

In vivo ROS production detected with the IVIS Lumina 2 was quantified using the FIJI software. The relative DHF-DA Integrated density was calculated for each mouse as the ratio of the integrated density obtained in mALA-treated skin relative to Light control area. For statistical comparison, the integrated density was normalized by calculating the ratio (vehicle/AA) for all possible pairs between AA and vehicle-treated animals for each time point. The average and standard error (SE) were represented and means of different time points were compared using analysis of variance.

For statistical analyses of gene expression data, an unpaired *t*-test was applied, setting $P \leq 0.05$ and fold change ≥ 2.0 as limits for significance. Quantitative real-time reverse-transcriptase–PCR data were analyzed using a comparative C_T method, by using 18S ribosomal RNA expression as an internal control. Gene expression fold changes were represented as the ratio between means of 2^{-Ct} values of mALA+Light and Light control groups mean values. Differentially expressed genes were selected on the basis of the Student's *t*-test comparison of means of 2^{-Ct} values between both groups.

For quantification of burn assays, day-to-day digital images were analyzed. The unhealed area was quantified using the FIJI software. The area under the curve was calculated separately for each mouse, and means were compared by the Student's *t*-test.

CONFLICT OF INTEREST

Clinical and commercial applications of the experimental procedures described in this work have been registered by a CSIC-UAM patent. The authors state no conflict of interest.

ACKNOWLEDGMENTS

JE was supported by Spanish MINECO grants SAF11-23493 and RTC-2014-2626-1 and Comunidad Autónoma de Madrid grant SkinModel CAM S10/ BMD-2359. DV and MRH were supported by US NIH grant R01AI050875. AJ was supported by Spanish MINECO grant FIS PI12/01253 and CAM S10/ BMD-2359. JCS was supported by Spanish MCINN grant CTQ2010-20870-C03-03. EC and MIC were supported by Spanish MECD-FPU and UAM-FPI fellowships, respectively. We thank Dr Colin Jahoda for the kind review of this manuscript. We thank biocellavi.com for assistance in the preparation of figures.

SUPPLEMENTARY MATERIAL

Supplementary material is linked to the online version of the paper at http:// www.nature.com/jid

REFERENCES

Baker RE, Murray PJ (2012) Understanding hair follicle cycling: a systems approach. Curr Opin Genet Dev 22:607–12

Bartosz G (2009) Reactive oxygen species: destroyers or messengers? Biochem Pharmacol 77:1303–15

Blanpain C, Fuchs E (2009) Epidermal homeostasis: a balancing act of stem cells in the skin. Nat Rev Mol Cell Biol 10:207–17

Blazquez-Castro A, Carrasco E, Calvo MI et al. (2012) Protoporphyrin IX-dependent photodynamic production of endogenous ROS stimulates cell proliferation. Eur J Cell Biol 91:216–23

Braun KM, Niemann C, Jensen UB et al. (2003) Manipulation of stem cell proliferation and lineage commitment: visualisation of label-retaining cells in wholemounts of mouse epidermis. Development 130:5241–55

Bylund J, Brown KL, Movitz C et al. (2010) Intracellular generation of superoxide by the phagocyte NADPH oxidase: how, where, and what for? Free Radic Biol Med 49:1834–45

Chiarugi P, Cirri P (2003) Redox regulation of protein tyrosine phosphatases during receptor tyrosine kinase signal transduction. Trends Biochem Sci 28:509–14

Choong ML, Tan AC, Luo B et al. (2003) A novel role for proliferin-2 in the ex vivo expansion of hematopoietic stem cells. FEBS Lett 550:155–62

Droge W (2002) Free radicals in the physiological control of cell function. Physiol Rev 82:47–95

el Bekay R, Romero-Zerbo Y, Decara J et al. (2007) Enhanced markers of oxidative stress, altered antioxidants and NADPH-oxidase activation in brains from Fragile X mental retardation 1-deficient mice, a pathological model for Fragile X syndrome. Eur J Neurosci 26:3169–80

Fassett JT, Nilsen-Hamilton M (2001) Mrp3, a mitogen-regulated protein/proliferin gene expressed in wound healing and in hair follicles. Endocrinology 142:2129–37

Fernandez V, Videla LA (1996) Biochemical aspects of cellular antioxidant systems. Biol Res 29:177–82

Giannoni E, Taddei ML, Chiarugi P (2010) Src redox regulation: again in the front line. Free Radic Biol Med 49:516–27

Gilhar A, Etzioni A, Paus R (2012) Alopecia areata. N Engl J Med 366:1515–25

Hamanaka RB, Glasauer A, Hoover P et al. (2013) Mitochondrial reactive oxygen species promote epidermal differentiation and hair follicle development. Sci Signal 6:ra8

Juarranz A, Jaen P, Sanz-Rodriguez F et al. (2008) Photodynamic therapy of cancer. Basic principles and applications. Clin Transl Oncol 10:148–54

Klebanoff SJ, Locksley RM, Jong EC et al. (1983) Oxidative response of phagocytes to parasite invasion. Ciba Found Symp 99:92–112

Le Belle JE, Orozco NM, Paucar AA et al. (2010) Proliferative neural stem cells have high endogenous ROS levels that regulate self-renewal and neurogenesis in a PI3K/Akt-dependant manner. Cell Stem Cell 8:59–71

Lopez-Pajares V, Yan K, Zarnegar BJ et al. (2013) Genetic pathways in disorders of epidermal differentiation. Trends Genet 29:31–40

Love NR, Chen Y, Ishibashi S et al. (2013) Amputation-induced reactive oxygen species are required for successful Xenopus tadpole tail regeneration. Nat Cell Biol 15:222–8

Machlin LJ, Bendich A (1987) Free radical tissue damage: protective role of antioxidant nutrients. FASEB J 1:441–5

Mates JM, Sanchez-Jimenez F (1999) Antioxidant enzymes and their implica-tions in pathophysiologic processes. Front Biosci 4:D339–45

Morris RJ, Liu Y, Marles L et al. (2004) Capturing and profiling adult hair follicle stem cells. Nat Biotechnol 22:411–7

Muller-Rover S, Handjiski B, van der Veen C et al. (2001) A comprehensive guide for the accurate classification of murine hair follicles in distinct hair cycle stages. J Invest Dermatol 117:3–15

Myant KB, Cammareri P, McGhee EJ et al. (2013) ROS production and NF-kappaB activation triggered by RAC1 facilitate WNT-driven intestinal stem cell proliferation and colorectal cancer initiation. Cell Stem Cell 12: 761–73

Perez VI, Bokov A, Van Remmen H et al. (2009) Is the oxidative stress theory of aging dead? Biochim Biophys Acta 1790: 1005–14

Pieczenik SR, Neustadt J (2007) Mitochondrial dysfunction and molecular pathways of disease. Exp Mol Pathol 83:84–92

Ramos R, Guerrero-Juarez CF, Plikus MV (2013) Hair follicle signaling networks: a dermal papilla-centric approach. J Invest Dermatol 133: 2306–8

Sena LA, Chandel NS (2012) Physiological roles of mitochondrial reactive oxygen species. Mol Cell 48:158–67

Serrels B, Serrels A, Mason SM et al. (2009) A novel Src kinase inhibitor reduces tumour formation in a skin carcinogenesis model. Carcinogenesis 30: 249–57

Speakman JR, Selman C (2011) The free-radical damage theory: accumulating evidence against a simple link of oxidative stress to ageing and lifespan. Bioessays 33:255–9

Valko M, Leibfritz D, Moncol J et al. (2007) Free radicals and antioxidants in normal physiological functions and human disease. Int J Biochem Cell Biol 39:44–84

Yuan J, Adamski R, Chen J (2010) Focus on histone variant H2AX: to be or not to be. FEBS Lett 584:3717–24